Quaternary Science Reviews 32 (2012) 131–142

Contents lists available at SciVerse ScienceDirect

Quaternary Science Reviews

journal homepage: www.elsevier.com/locate/quascirev

The East Asian winter monsoon over the last 15,000 years: its links to high-latitudes and tropical climate systems and complex correlation to the summer monsoon

Luo Wang [a,*], Jingjing Li [b], Houyuan Lu [a], Zhaoyan Gu [a], Patrick Rioual [a], Qingzhen Hao [a], Anson W. Mackay [c], Wenying Jiang [a], Binggui Cai [a], Bing Xu [a], Jingtai Han [a], Guoqiang Chu [a]

[a] *Key Laboratory of Cenozoic Geology and Environment, Institute of Geology and Geophysics, Chinese Academy of Sciences, Beijing 100029, China*
[b] *School of Geosciences and Resources, China University of Geosciences, Beijing 100083, China*
[c] *Environmental Change Research Centre, Department of Geography, University College London, London WC1E 6BT, UK*

A R T I C L E I N F O

Article history:
Received 24 May 2011
Received in revised form
29 October 2011
Accepted 4 November 2011
Available online 25 November 2011

Keywords:
East Asian winter monsoon
Diatom
Holocene
Arctic oscillation
Siberian High
El Niño
East Asian summer monsoon
Australian summer monsoon
Huguang Maar Lake

A B S T R A C T

The East Asian winter monsoon (EAWM) not only plays an important role within the Asian climate system, but also carries cold air from the high northern latitudes across the Equator to the Southern Hemisphere, acting as a link between the polar and tropical climate systems. However, past changes of the EAWM have not been clearly established so far due to the lack of suitable proxy records. Here, we at first establish an index of the EAWM by comparing the results of a sediment trap experiment and 100-year sedimentary record from Huguang Maar Lake (HML) with modern records of the EAWM, Siberian High (SH) and Arctic Oscillation (AO). Secondly, we present a continuous record of the strength of the EAWM for the past 14,500 years based on sedimentary diatom assemblages in HML. The record is derived from fluctuations in the relative abundance of two planktonic diatom species. The link with the EAWM intensity is through high wind speeds inducing turbulent mixing, which stimulates the productivity of the meroplanktonic species *Aulacoseira granulata*. The diatom record of the past 14,500 years shows that the EAWM shifted from strong to weak from the early to late Holocene. This linked to both changes in winter temperature at high-latitudes and in El Niño conditions in the tropics. Our record shows that the EAWM and East Asian summer monsoon (EASM) as recorded in stalagmites, were in-phase instead of anti-correlated on orbital time scales during the Holocene. On a millennial time scales, the EAWM was anti-phase with the EASM during the Last Glacial–Holocene transition. However, during the early–middle Holocene the relationship between the EAWM and EASM shows spatial variations. In northern China, the records show significant anti-phase, but in southern China the anti-phase was not observed. During the late Holocene, we did not find any clear relationship between the EAWM and EASM. We also explored the link between the EAWM and the Australian summer monsoon (ASM). Anti-phase of the ASM with summer insolation in the Southern Hemisphere is an enigmatic exception that cannot be explained by the classic theory of insolation. During early Holocene the EAWM was in-phase with the Australian summer monsoon (ASM), which provides the first direct evidence to support the hypothesis that the intensity of the EAWM affected, at least in part, the strength of the ASM.

1. Introduction

The East Asian winter monsoon (EAWM) is one of the most active components in the global climate system. It generally refers to the atmospheric flow over Asia associated with movement of cold air coming from the Siberian High (SH) (Fig. 1) (Chen et al., 1991; Ding, 1994; Huang et al., 2003, 2007; Chan and Li, 2004; Chang et al., 2006). The SH, also called Siberian anticyclone, is a semi-permanent system of high atmospheric pressure centered in northeastern Siberia during the colder half of the year, when the air temperature near the center of the high-pressure cell is often lower than −40 °C. The SH affects the weather patterns in the higher latitudes of the Northern Hemisphere, it is responsible both for severe cold and dry conditions in winter across Siberia and most of China (Oliver, 2005). The variability of the EAWM depends largely on the behavior of the SH (Gong and Ho, 2002) and Arctic

* Corresponding author. Tel.: +86 10 82998261; fax: +86 10 62032495.
E-mail address: wangluo@mail.iggcas.ac.cn (L. Wang).

0277-3791/$ – see front matter © 2011 Elsevier Ltd. All rights reserved.
doi:10.1016/j.quascirev.2011.11.003

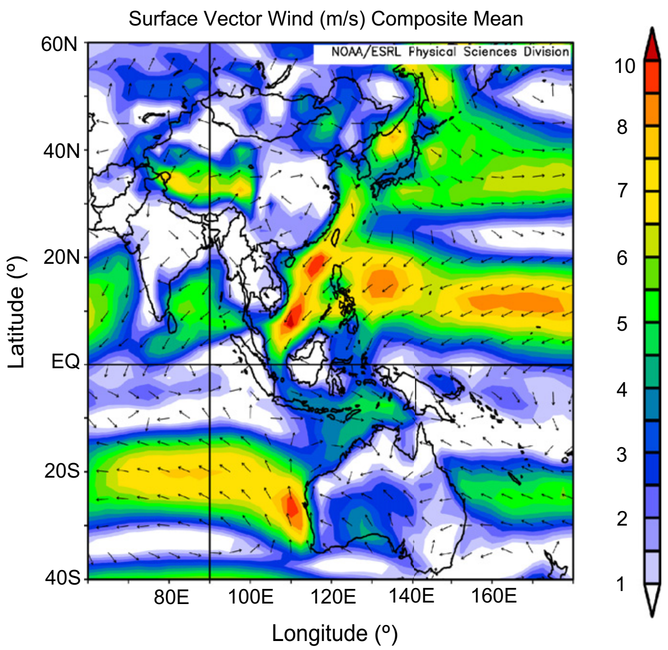

Fig. 1. The characteristics of surface winds of January (based on the NCEP/NCAR reanalysis data) (Kalnay et al., 1996). To best illustrate the path of surface winds we chose data from 1960 to 1985 AD, as this interval corresponds with strong winter monsoon. HML means the location of Huguang Maar Lake.

Oscillation (AO) (Gong et al., 2001). AO was introduced as an annular mode of atmospheric circulation by Thompson and Wallace (1998). Fluctuations in the AO create a seesaw pattern in which atmospheric pressure and mass in northern polar and mid-latitudes alternate between positive and negative phase (Wallace, 2000). When the AO is in a negative phase and the SH is strong, the temperature is cold at high northern latitudes, resulting in a strong EAWM (D'Arrigo et al., 2005). In addition, the EAWM have been linked to the El Niño/Southern Oscillation (ENSO) (Li, 1990; Li and Mu, 2000; Wang et al., 2000; Xu and Chan, 2001; Wang et al., 2008a). A weak EAWM usually occurs during an El Niño year, but the reverse occurs during a La Niña year (Li, 1989).

When the EAWM shifts southward, it not only covers northern China and Japan (Chen et al., 2005; Wang et al., 2009), but its southern branch also forms northeasterlies which penetrate through the South China Sea and across the tropics into the Southern Hemisphere (Fig. 1) (Suppiah and Wu, 1998; Gong and Ho, 2002; Jhun and Lee, 2004; Miller et al., 2005). The EAWM therefore, not only influences the East Asian summer monsoon (EASM), but also affects convection over the maritime continent and the Australian summer monsoon (ASM) (Chen et al., 1991; Suppiah and Wu, 1998). It is necessary therefore for us to improve our knowledge of the EAWM in order to understand climate dynamics in this vast region.

So far, most of our knowledge on past changes of the EAWM comes from loess records from the Chinese Loess Plateau. The grain size of loess have been used as an indicator to reconstruct the changes of the EAWM on orbital and millennial time scales (An et al., 1991a; Porter and An, 1995; Xiao et al., 1995; An and Porter, 1997; Liu and Ding, 1998; Liu et al., 1999; Ding et al., 2002; Lu et al., 2004; Porter and Zhou, 2006). When the EAWM is strong, it carries coarse dust to the Chinese Loess Plateau resulting in the increase of the grain size in loess records (An et al., 1991a). On orbital time scales, changes in the EAWM have been linked to changes in ice volume in the Northern Hemisphere (Ding et al., 1995; Liu and Ding, 1998; Porter, 2001), which is primarily controlled by the Northern Hemisphere summer insolation at 65°N (Hays et al., 1976; Imbrie et al., 1984; Ruddiman et al., 1989; Shackleton et al., 1990). The view is that the Northern Hemisphere ice sheets indirectly influenced the EAWM by exerting an important control on the intensity of the SH. During glacial, the large ice sheets resulted in cold surface conditions in Siberia and strong SH that lead to strong EAWM. In contrast, during interglacial small ice sheets resulted in weak SH and weak EAWM. During the Holocene, the grain size of many Chinese loess records (Yang and Ding, 2008) and the high-resolution record of titanium concentration from the Huguang Maar Lake (HML) (Yancheva et al., 2007) indicate that the EAWM strengthened through time from low intensity during the warm early Holocene to high intensity during the cool late Holocene. However, it has been shown that Northern Hemisphere ice sheets in land were larger during the early–middle Holocene than during the late Holocene (Dyke and Prest, 1987; Kutzbach et al., 1998). The winter insolation in Northern Hemisphere is lower during early Holocene than during late Holocene (Berger and Loutre, 1991). Such change in the size of ice sheets and the insolation should have caused a weakening of the EAWM from the early to late Holocene. This contradiction needs to be explored.

Recent studies indicated that the grain size of loess not only was controlled by the EAWM, but was also influenced by the EASM, which controls the advance or retreat of the boundaries between the areas of desert and loess (Yang and Ding, 2008). Therefore, it is still open to debate whether the grain size in loess records is a robust index of the EAWM strength. The reliability of the titanium record from the HML as an indicator of the EAWM (Yancheva et al., 2007) has also been questioned. This is because titanium may not be carried by winter winds from the Chinese Loess Plateau, but may be derived from erosion by rainfall running off the HML catchments or water level changes (Zhou et al., 2007, 2009). Another index for reconstructing changes in the EAWM has been derived from the west–east/north–south gradients in sea surface temperatures established for the northern part of the South China Sea (Tian et al., 2010; Huang et al., 2011). However, these marine sediment records compared to lake records have a rather low temporal resolution over the Holocene.

There is therefore a clear need to develop a new, high-resolution, independent proxy record of the EAWM. Wang et al. (2008b) used high-resolution diatom assemblages as a proxy indicator of the EAWM from HML in subtropical China during the Lateglacial–early Holocene transition. Here we expand on that study, by reconstructing the EAWM from the late Last Glacial (14.5 ka BP) through the complete Holocene sequence up to the present using the same sediment core. We provide new, additional evidence linking diatom assemblage change to winter monsoon through extended sediment trap studies, and the comparison of diatom assemblages with indices of the SH and AO over the last c. 110 years. We discuss the correlation between the EAWM and EASM on orbital and millennial time scales, and possible linkages to the EAWM and Australian summer monsoon (ASM).

2. Geographical setting

HML (21°9′N, 110°17′E, Fig. 2) is located in Guangdong Province, near the coast of South China Sea. HML is a crater lake, with a diameter of ~1.7 km and a maximum depth of ~20 m. This lake is influenced by both the Asian summer and winter monsoons (Fig. 2). During winter, the strong EAWM covers northern China and bifurcates south with one branch flowing along the coast of East Asia (Lau and Li, 1984; Ding, 1994; Chen et al., 2000, 2005; Wang et al., 2009). Therefore, the EAWM winds blowing over HML come from the northeast (Fig. 1). These are responsible for the complete mixing of the HML water column. During summer, by contrast, the lake strongly stratifies due to weak winds and high temperatures (Wang et al., 2008b).

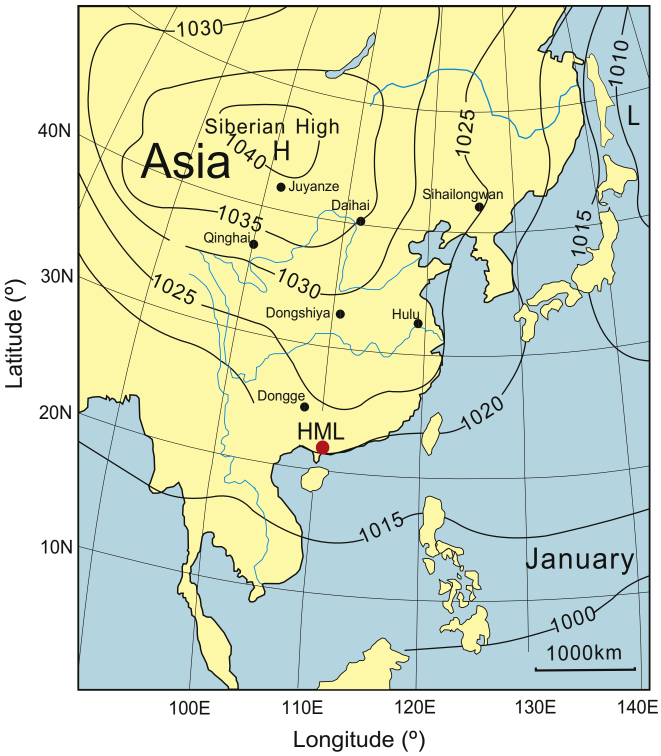

Fig. 2. Location of the Huguang Maar Lake (HML) and other sites in China with records of the monsoon for comparison: Qinghai Lake (Chen et al., 2005), Juyanze Lake (Chen et al., 2003; Hartmann and Wünnmann, 2009), Daihai Lake (Li et al., 2004; Xiao et al., 2004; Xiao et al. 2008), Sihailongwan Maar Lake (Schettler et al., 2006; Parplies et al., 2008; Stebich et al., 2009), Dongshiya Cave (Cai et al., 2008), Hulu Cave (Wang et al., 2001) and Dongge Cave (Dykoski et al., 2005). The isobar line is mean sea-level pressure (hPa) (after Zhang and Lin, 1992).

The strong contrasting seasonal change in the lake water mixing regime makes HML an ideal setting for the reconstruction in the strength of the EAWM due to: (i) the site is located in the path of the EAWM before it crosses the Equator and influences the Intertropical Convergence Zone (ITCZ) which in turn influences the EASM; (ii) it is far from Siberia, so it is suitable for testing if changes in the EAWM at low latitudes are in-phase with changes in the SH and in Northern Hemispheric climate over the vast Chinese mainland; (iii) this lake is a highly sensitive recorder of past climate in the tropical zone, because changes in its physical properties, such as lake turnover and stratification, are influenced by seasonal monsoon variability (Wang et al., 2008b).

3. Materials and methods

In 1997, seven sediment cores (HUG-A to HUG-G) from three different sites in HML were drilled with a high precision piston coring system (Mingram et al., 2004). The Core HUG-B used for this study has a length of 24.28 m and was recovered from a water depth of 13.4 m (Mingram et al., 2004). The age model is based on 9 AMS (accelerator mass spectrometry) ^{14}C dates, 5 of leaves and 4 of bulk sediment. Details of the age model are given in Yancheva et al. (2007), and all the ages given here are calibrated ages. The piston core we study here covers the last 14,500 years.

Two approaches were used to demonstrate how seasonal changes in diatom assemblage are associated with the East Asian winter monsoon. First, monthly sediment traps samples were collected from the lake between August 2007 and March 2009. Cylindrical sediment traps were built according to the recommendations of Blomqvist and Hakanson (1981). The traps were deployed for one month between the 9th of each month at about 16 m water depth in the center of the lake. The solid material together with water in the cups of trap were transported to the laboratory for diatom analysis. The lake water temperature profile was monitored using thermistors (Vemco) at 2 h interval from November 2007 to May 2008. The changes in diatom composition were compared with meteorological data spanning the period between August 2007 and March 2009 from Zhanjiang City close to HML.

Second, a short gravity core was retrieved in August 2007 from the deepest part of the lake using a UWITEC gravity corer (30-cm long) and sectioned into 0.5–1 cm intervals. The activities of ^{137}Cs, ^{210}Pb, and ^{226}Ra were measured by gamma spectrometry using a low-background well-type germanium detector (EGPC 100P-15R) at the Institute of Geology and Geophysics, Chinese Academy of Sciences, Beijing. The chronology derived from the ^{210}Pb CRS model matches with the peak of ^{137}Cs and shows that this core spans the last ca 110 years (Fig. 3). Diatom assemblages were analyzed and our diatom-based EAWM index was validated by comparison with meteorological records of the EAWM index (Wang et al., 2009) and SH index (D'Arrigo et al., 2005; Panagiotopoulos et al., 2005).

Diatom slides were prepared using conventional method. Approximately 0.05 g of dry sediment from each sample was heated with H_2O_2 followed by HCl to remove organic matters and carbonates, respectively (Battarbee et al., 2001; Li et al., 2009). Between 300 and 600 diatom valves were counted from each sample (with the exception of the samples taken at 64, 134, 844 and 896 cm core depth that had low-diatom concentration and for which only about 200 valves were counted). Valves were identified to species level with the assistance of floras including Krammer and Lange-Bertalot (1986–1991). Diatom data were expressed as percent relative abundance of the total number of valves counted in each sediment sample. Wang et al. (2008b) used the ratio of two species as an indicator of the EAWM for the period 17,500–6000 cal. yrs BP: *Cyclotella stelligera* to *Aulacoseira granulata* (S/G). In this study, for convenience, we use the inverse AG/CS ratio (*A. granulata*/*C. stelligera*), as a positive index for the strength of the EAWM at the HML. Diatom concentrations (valves per gram) for each level were estimated by the addition of divinyl benzene microspheres to cleaned suspensions (Battarbee and Kneen, 1982).

4. Results and discussion

4.1. Proxy records of the East Asian winter monsoon

The strong relationship between diatom assemblages at the HML and winter monsoon winds (WMW) was previously investigated by Wang et al. (2008b). In this study we further explore the possibility of using diatom assemblages as a proxy for the EAWM. Here we show detailed seasonal change using monthly diatom, water chemistry and water stratification data, and compare the changes in diatom assemblage data over the past 100 years with the modern EAWM index (Wang et al., 2009) and SH index (D'Arrigo et al., 2005; Panagiotopoulos et al., 2005).

4.1.1. Seasonal changes in diatom assemblages, nutrient concentrations and water stratification

Patterns in dominant diatom species from the monthly sediment trap samples from the HML show distinct seasonal changes (Fig. 4a and b). Previous studies on diatom ecology have shown that *Cyclotella* taxa are euplanktonic species, which most commonly occur when lakes are thermally stratified during warm periods with weak wind (Battarbee et al., 2002; Sorvari et al., 2002; Rühland et al., 2003). *Cyclotella* species are also commonly

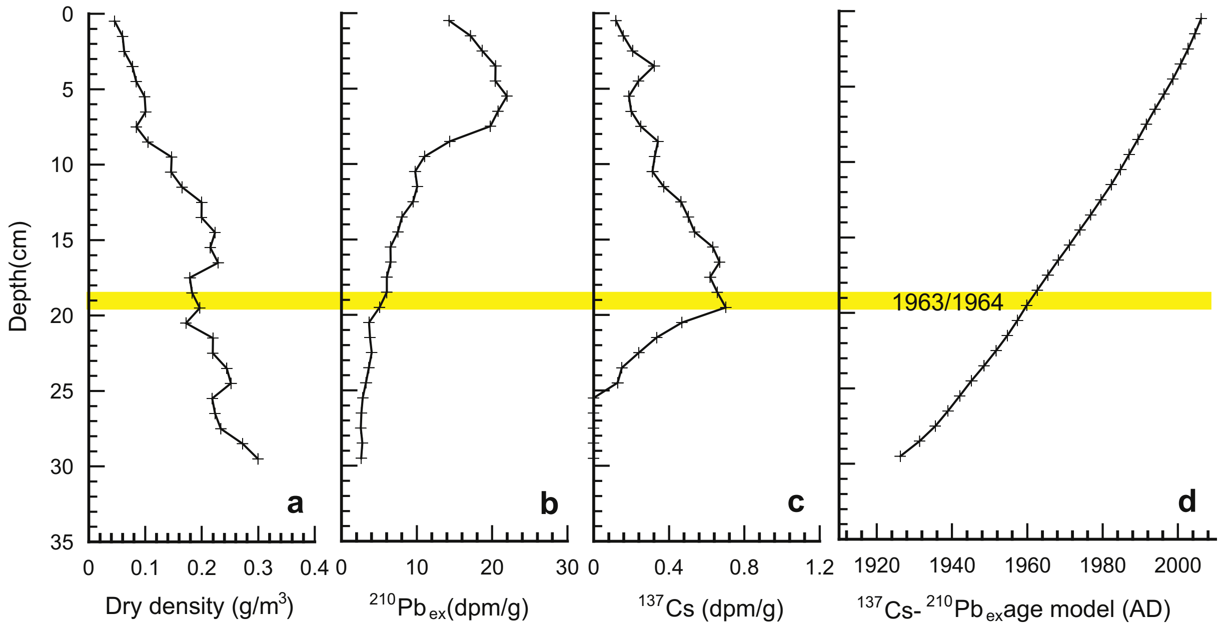

Fig. 3. HML short core ^{137}CS–^{210}Pb$_{ex}$ age model diagram. a. Dry bulk density of sediment. b and c. Concentrations of ^{210}Pb and ^{137}Cs. d. ^{210}Pb and ^{137}Cs age model.

observed in higher abundances in lakes with low nutrients (i.e. oligotrophic) (Rühland et al., 2003). During summer, high temperatures and weak winds (Fig. 4c) promote thermal stratification of the lake water column (Fig. 5), when nutrients (N and Si) are low (Fig. 4d and e). These conditions favor the development of euplanktonic and oligotrophic *Cyclotella* species in HML (Fig. 4b).

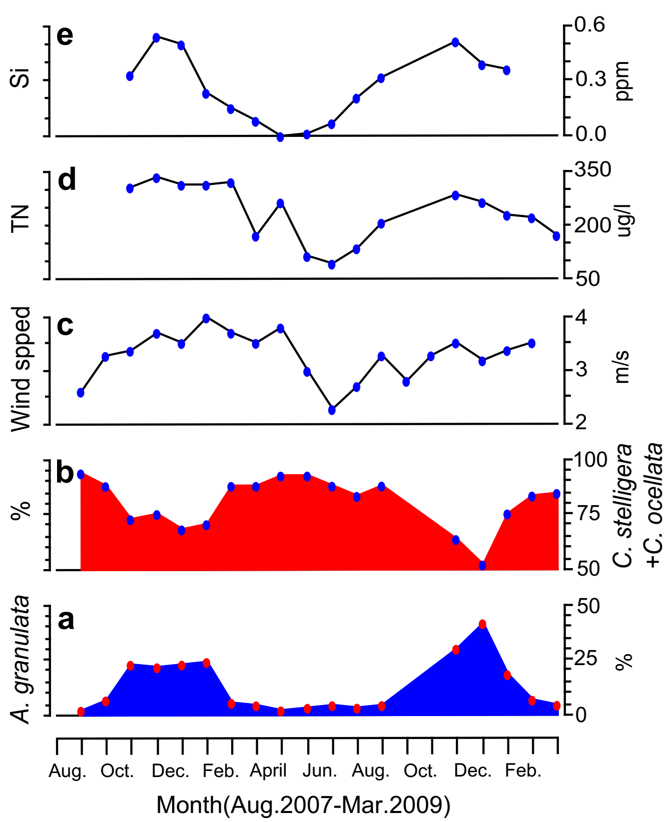

Fig. 4. Relative abundance of diatoms in sediment trap samples, water chemistry of HML and wind speed diagram. a and b. Relative percentages of *Aulacoseira granulata* and *Cyclotella stelligera* + *ocellata*. c. Mean monthly wind speed from Zhanjiang meteorological station from 8/2007 to 3/2009. d and e. Monthly concentrations of total nitrogen and silica in HML surface water every month from 11/2007 to 3/2009. The trap samples for Sep. and Oct. 2008 were lost.

In contrast, many *Aulacoseira* species are meroplanktonic species. Meroplanktonic organisms enter the plankton when mixing conditions are such that they can be suspended and maintained in the water column (Kilham, 1990). *Aulacoseira* species, such as *A. granulata*, also appear to have rather high nutrient requirements (Kilham and Kilham, 1975). During periods of strong wind, the lake thermal stratification breaks down, causing nutrient-rich bottom water to mix with surface water and therefore offering conditions for meroplanktonic diatoms to thrive in abundance. Therefore, the abundance of *Aulacoseira* species, such as *A. granulata*, is an indirect paleoenvironmental indicator of the persistence of strong, seasonal wind stress and resultant turbulent water column mixing and nutrient upwelling conditions (Pilskaln and Johnson, 1991). During winter in the HML region, the EAWM regime is dominant with high wind speeds inducing turbulent mixing which result in an isothermal water column (Fig. 5) (Wang et al., 2008b). These conditions lead to nutrient-rich lake water favoring meroplanktonic and eutrophic diatoms, such as *A. granulata* (Fig. 4a).

Thermistor data for 2008–2009 recorded the rapid development of thermal stratification in HML from the middle of February 2008 (Fig. 5). The onset of thermal stratification corresponded to a decline in the abundance of *A. granulata* from the beginning of spring, although winds were still strong until May that year (Fig. 4c). These data show how *A. granulata* which has strongly silicified cells is too heavy to remain in suspension in the photic zone as stratification develops. Unless winter monsoon lasts into the spring season and is strong enough to prevent the establishment of thermal stratification, a heavily-silicified diatom such as *A. granulata* will not be able to remain in suspension and will sink out from the water column of HML. The dependence of this species on mixing conditions has been reported by Kilham (1990). Stability of thermal stratification in lakes is greatly affected by wind speed. In particular, Langmuir circulations are elongated, wind-induced convection cells that form at the surface of lakes and of the sea (Langmuir, 1938). Importantly, Langmuir circulation develops only when wind speed exceeds a threshold of 3 m/s (Scott et al., 1969; Assaf et al., 1971; Reynolds, 2006). It should be noted that the relationship between the relative abundance of

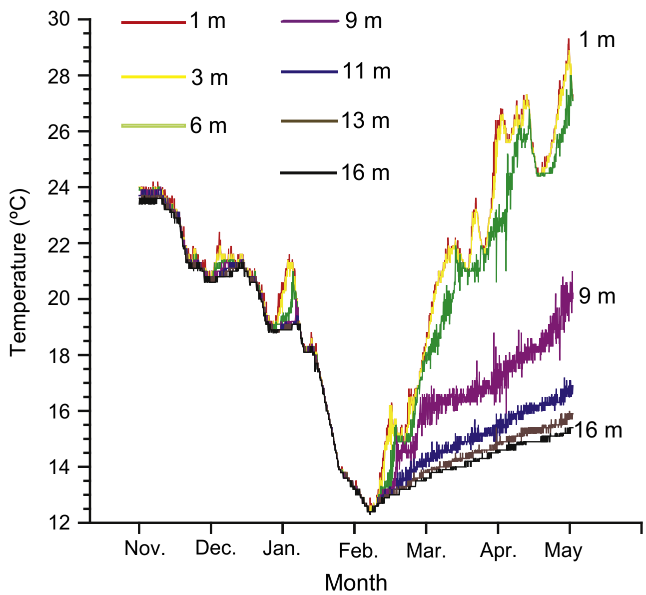

Fig. 5. Lake water temperature profiles for November 2008–May 2009. Temperatures indicate that the water column was nearly isothermal during the winter. At the beginning of spring water stratification started to develop due to increasing temperature, and became fully established from the beginning of March.

A. granulata and wind speed is not linear and cannot be expressed quantitatively.

This seasonal alternation between stratification and isothermy is reflected in changes in diatom assemblages in sediment traps from HML (Fig. 4). An increase in thermal stability will favor the small, planktonic *C. stelligera* that has low sinking rates and that prefers low nutrient environments, resulting in high relative abundance of this species in sediment traps during summer months. A well mixed water column will favor the heavily-silicified *A. granulata* that requires turbulence, higher nutrient levels and tolerates lower light conditions, resulting in high relative abundance of this species in sediment traps during windy winter months in the HML.

4.1.2. Sedimentary diatom assemblages over the past 100 years and link to the EAWM, SH and AO indices

The linkages between the EAWM and the SH and AO have been established from the meteorological records (Gong et al., 2001; Wu and Wang, 2002; Jhun and Lee, 2004; Chen et al., 2005; Chang et al., 2006; Kang et al., 2006). Instrumental measurements show that the EAWM has significantly weakened after the 1980s (Chang et al., 2006; Kang et al., 2006; Wang et al., 2009; Wang and Chen, 2010). Wang and Chen (2010) elaborates on the meanings of 18 existing EAWM strength indices and classifies them into four categories: low-level wind indices, upper zonal wind shear indices, east–west pressure contrast indices, and East Asian trough indices. In this paper, we compare our data with East Asian trough indices, which use the strength of the 500-hPa East Asian trough as indicative of the EAWM. Winter monsoon velocity at Xisha in the South China Sea (16°50′N, 112°20′E) also shows a similar weakening trend after the 1980s (Liu et al., 2008). This change in the late 1980s (Fig. 6d) is concomitant with a shift to a weaker SH (Fig. 6e and f) as shown by D'Arrigo et al. (2005) and Panagiotopoulos et al. (2005), who made use of wintertime [December–January–February (DJF)] means of both historical gridded analyses of sea-level pressure (SLP) and individual station observations of SLP and surface pressure to define their index. Following the 1980s, winters in northern Europe became warm due to a shift in the AO from a negative to a positive phase (Fig. 6g) (Thompson and Wallace, 1998). Warmer European winters resulted in a weaker SH, and through reduced snow cover extent, caused a decline in the strength of the EAWM (Barnett et al., 1988; Clark et al., 1999; Clark and Serreze, 2000).

The diatom sedimentary record over the last 100 years from the HML shows two abrupt shifts. In the late 1980s, a marked decrease in *A. granulata* and a change in the AG/CS ratio (Fig. 6b and c) matched the decline in the EAWM strength at about 1986 AD (Chang et al., 2006; Kang et al., 2006; Wang et al., 2009) (Fig. 6d), the decrease in the strength of the SH (Fig. 6e and f) and the shift in AO from a negative to a positive phase (Fig. 6g). The abrupt increase in *A. granulata* and AG/CS (Fig. 6b and c) at about 1920 AD also

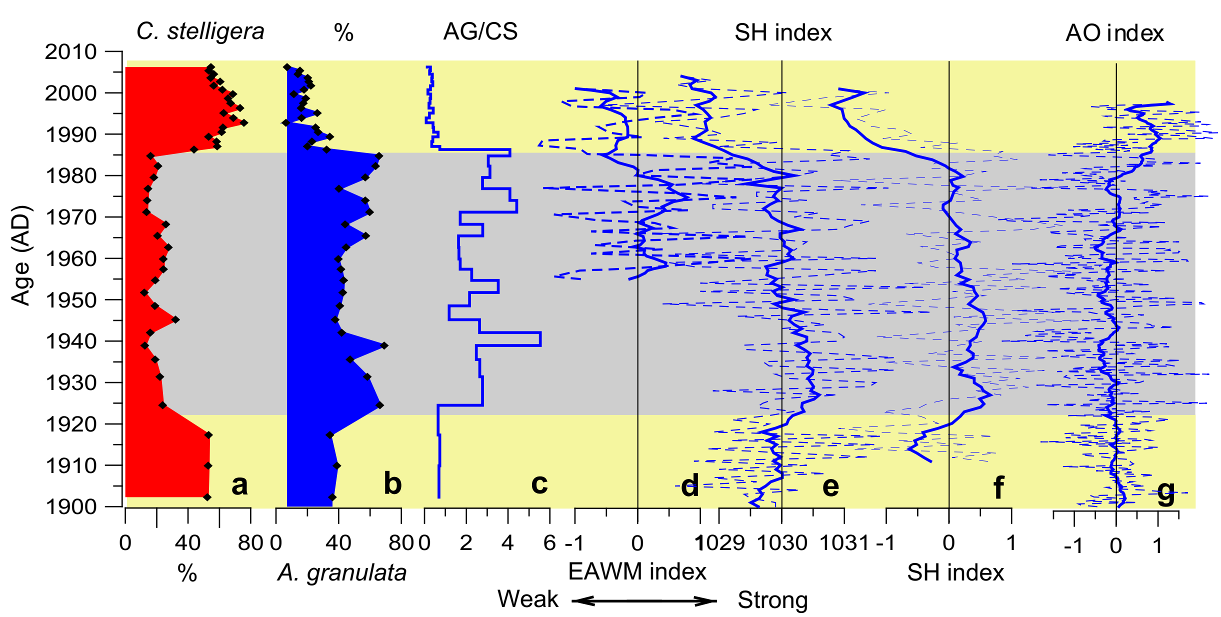

Fig. 6. The HML diatom record for the past 100 years. a and b. Percentage diagrams of *C. stelligera* and *A. granulata*; c. the ratio of AG/CS (AG: *A. granulata*, CS: *C. stelligera*); d. the EAWM index (Wang et al., 2009); e and f. the Siberian High index (D'Arrigo et al., 2005; Panagiotopoulos et al., 2005); g. Arctic Oscillation index (Thompson and Wallace, 1998); the shaded areas represent intervals with strong EAWM.

matches with changes in the SH and AO indices. These data indicate that the diatom assemblages not only record the changes in the EAWM seasonally (Fig. 4), but also on a decadal time scales.

Thus, the results from the diatom analysis of trap and short core samples demonstrate that the diatom *A. granulata* abundance and the ratio of AG/CS can be used as an indicator of the EAWM, with high/low values of the ratio indicating strong/weak EAWM (Fig. 6).

4.2. Inference of the EAWM intensity from the diatom record for the past 14.5 ka years

In our 14.5-ka-long record, *A. granulata* and *C. stelligera* are the main diatom species, although benthic, littoral, diatoms are also periodically important as a group (Fig. 7). It must be noted that abundances of benthic follow that of *A. granulata*. This suggests that their presence in middle of lake at the coring point is also driven by strong mixing. The will not be discussed further in this paper. Between 13 and 5 ka, the relative abundance of *A. granulata* and the ratio of AG/CS showed high values indicating strong EAWM during this period (Fig. 7). Relative abundance values of *A. granulata* and the AG/CS ratio exhibit three peaks during this period. However, after ∼5 ka years, the relative abundances of *A. granulata* and the AG/CS ratio decreased (Fig. 7) and abundances of *C. stelligera* increased (Fig. 7), indicating a dramatic reduction in the EAWM. During the late Holocene, two small peaks of AG/CS occur at c. 3000 and after 1000 cal. yrs BP, indicating episodes with slightly enhanced EAWM.

4.3. Linkage between the EAWM and winter climate changes at high-latitudes and in tropical regions

4.3.1. Links to high-latitudes climate changes

The HML diatom record shows that the EAWM shifted from strong to weak from the early to late Holocene. The change is consistent with winter (December) insolation increasing from the early Holocene to late Holocene (Berger and Loutre, 1991) (Fig. 8d) and with reconstructed European winter temperatures (Davis et al., 2003). High-resolution records from the Holzmaar and Meerfelder maar lakes in Germany also show that the winter season was colder in the early–middle Holocene than in the late Holocene (Litt et al., 2009) (Fig. 8b and c). Cold winters in the early Holocene in the Northern Hemisphere would have promoted strong SH resulting in strong EAWM as recorded by diatom assemblages from the HML, which is characterized by high values of *A. granulata* (Fig. 7) and the ratio AG/CS (Fig. 8a). In contrast, warm winters during the late Holocene in the Northern Hemisphere would have caused weak SH resulting in weak EAWM as indicated by low values of the percentage of *A. granulata* and the ratios of AG/CS from the HML.

On millennial time scales and over the course of the Holocene, we recognize four events with strong EAWM that occurred during the intervals 10,000–8500, 7000–5500, 3100–2500, 1000–500 cal. BP (Fig. 8a). The changes in strength of the EAWM were roughly consistent with changes in the intensity of atmospheric circulation of SH as indicated by K^+ concentration from the GISP2 ice-core (Mayewski et al., 1997; Meeker and Mayewski, 2002) (Fig. 8f). High K^+ deposition are associated with spring strengthening of the SH, the coldest air mass in the Northern Hemisphere, and deepening of the low over South Asia (Meeker and Mayewski, 2002). The EAWM events during the periods 10–8.5 ka and 7–5 ka are also consistent with the decrease in European winter temperatures (Litt et al., 2009) (Fig. 8b and c).

4.3.2. Links to climate changes in tropical regions

Besides high-latitudes changes impacting on the EAWM, tropical climate changes are also important (Li, 1989; Wang et al., 2000; Wang et al., 2008a). Meteorological studies showed that a weak EAWM usually occurs during the developing phase to the mature phase of an El Niño year, and that the reverse occurs during a La Niña year (Li, 1989). The relationship between El Niño-Southern

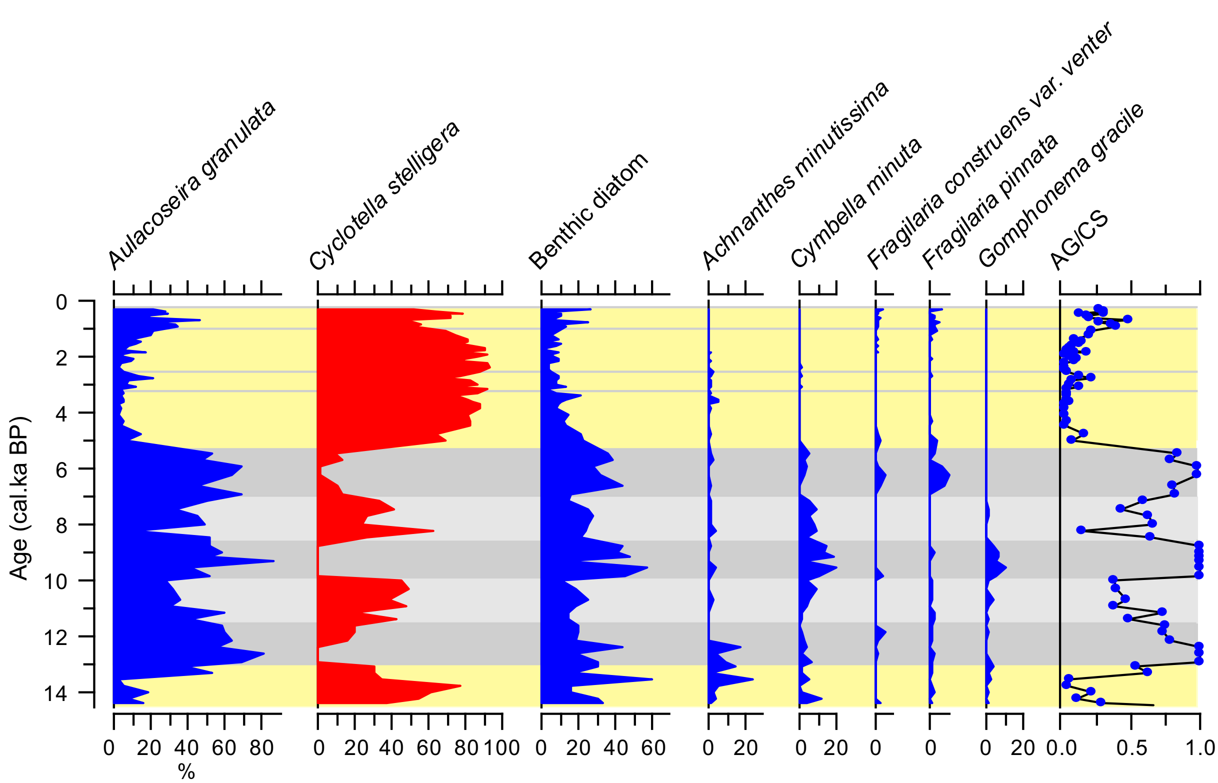

Fig. 7. Percentages of the two main diatom species over the past 14.5 ka cal. BP, AG/CS stands for the ratio between *A. granulata* and *C. stelligera* and it is used as an indicator of the EAWM. Shaded bars represent strong EAWM.

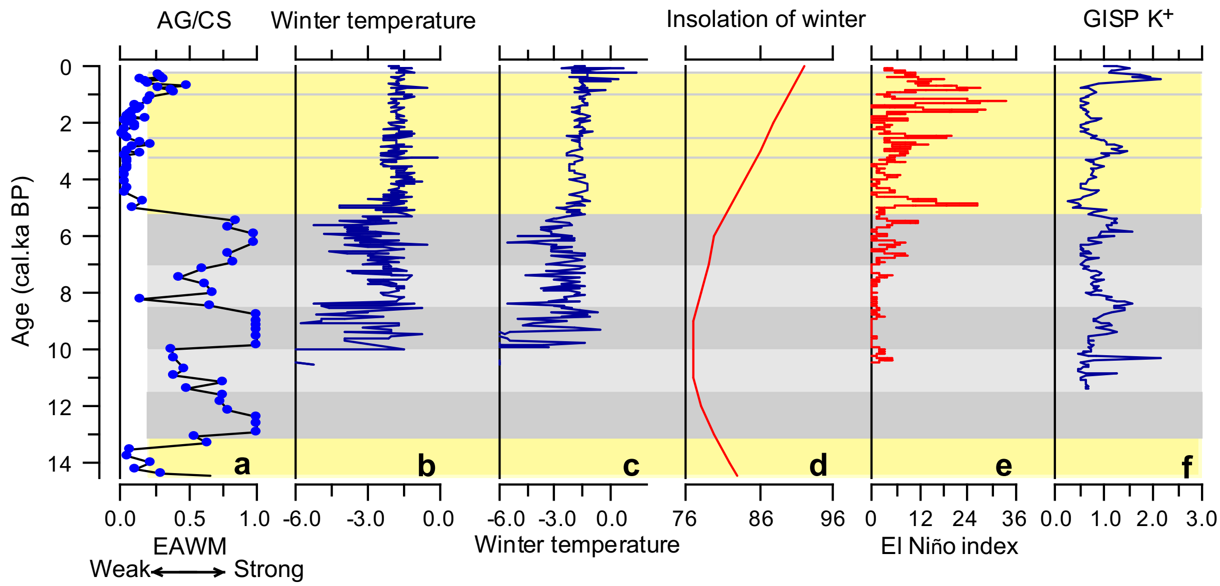

Fig. 8. The HML EAWM record compared with high-latitudes and tropical climate changes. a. AG/CS ratio; b and c. winter temperature records from Meerfelder maar lake and Holzmaar Lake, Germany, respectively (Litt et al., 2009); d. December (China winter) insolation at 60° N (W/m^2) (Berger and Loutre, 1991); e. El Niño events per 100 years (Moy et al., 2002); f. Siberian High index (Mayewski et al., 2004). Shaded bars indicate strong EAWM.

Oscillation (ENSO) and the Asian winter monsoon is bridged by an anomalous lower-tropospheric anticyclone located in the western North Pacific (Wang et al., 2000).

The ENSO cycle has been a feature of the Earth's climate for at least the past 130,000 yrs (Tudhope et al., 2001), but there is a systematic difference between the early–middle Holocene and the last 5000 yr, as indicated in various Holocene ENSO records (Rodbell et al., 1999; Moy et al., 2002; Conroy et al., 2008). According to these records, at 5 ka there was an increase in the frequency of El Niño events (Rodbell et al., 1999; Tudhope et al., 2001; Moy et al., 2002) (Fig. 8e). Moy et al. (2002) suggested that the shift perhaps was due to changes in boreal summer insolation, which is consistent with a modeling study (Clement et al., 2000). During El Niño, anomalous Philippine Sea anticyclone is induced by both the in situ ocean surface cooling and the subsidence forced remotely by the central Pacific warming. The anomalous anticyclone is associated with strong southerly winds penetrating along the east Asian coasts and significantly weakening the EAWM (Wang et al., 2000). Therefore, during the late Holocene more frequent and stronger El Niño events may be an important factor, leading to the shift in the strength of the EAWM from strong to weak at around 5 ka years as indicated by the ratio of AG/CS (Fig. 8a).

On millennial time scales our EAWM record as the ratio of AG/CS indicated only two events with intense EAWM during the late Holocene (Fig. 8a) whereas the record of El Niño events shows a series of large fluctuations during the late Holocene (Fig. 8e), indicating an inconsistent relationship between the EAWM and ENSO. This variability of the high-latitudes (SH)-tropical (ENSO) teleconnection had also been found when comparing SH series with ENSO over the past thousands years (D'Arrigo et al., 2005). It is likely that other factors influence the relationship between the ENSO and the EAWM during the late Holocene, such as the Pacific Decadal Oscillation (PDO) (Wang et al., 2008a). Meteorological observations indicate that when the PDO is in its high phase, there is no robust relationship between ENSO and EAWM on an inter-annual time scale, and when the PDO is in its low phase, ENSO exerts a strong influence on the EAWM (Wang et al., 2008a).

In summary, while the EAWM as recorded by diatoms from the HML is controlled by high latitude climate change, it is also affected by tropical climate changes (El Niño). The significant shift in winter temperatures from cold to warm (Litt et al., 2009) (Fig. 8b and c) together with the systemic changes in the ENSO cycle at around 5 ka are most likely the two main reasons for the abrupt shift toward weak EAWM conditions observed at about 5 ka BP from the HML.

4.4. Correlation between the EAWM and EASM

4.4.1. Orbital time scales

On orbital time scales, loess records indicate that the EAWM is negatively correlated with the EASM (Ding et al., 1995; Liu and Ding, 1998; Porter, 2001). In details, the grain size of loess have been used as an index of the EAWM (An et al., 1991a; Liu and Ding, 1998; Liu et al., 1999) and magnetic susceptibility of loess as an index of the EASM (Kukla and An, 1989; An et al., 1991b). The EASM record in the Chinese loess-soil sequences show glacial and interglacial cycles (Ding et al., 1995; Liu and Ding, 1998; Porter, 2001; Lu et al., 2004; Hao and Guo, 2005) because the EAWM has an important influence on the EASM (Ding et al., 1995; Liu and Ding, 1998; Porter, 2001).

The abundance of *A. granulata* and the ratio of AG/CS show that the EAWM decreased from the early–middle Holocene to late Holocene in the HML (Fig. 7), when the EASM also decreased as indicated by pollen data from HML (Wang et al., 2007a). Various records of the EASM also show a similar trend. For example, in southern China, the oxygen isotope records from stalagmites suggest a decrease in strength of the EASM (Fig. 9d) (Dykoski et al., 2005; Wang et al., 2005). It is however open to debate whether the stalagmite oxygen isotope records are a reliable proxy of summer monsoon (see Tan (2009) and Clemens et al. (2010) for in depth discussion on this issue). In northern China, the pollen data from Daihai Lake (Li et al., 2004; Xiao et al., 2004) (Fig. 9e) and Bayanchagan Lake (Jiang et al., 2006, 2010) indicated a decrease of the EASM for the same interval. At the northern margin of the EASM an obvious decrease of the EASM intensity was suggested for the late Holocene on the basis of aeolian records from eastern Inner Mongolia (Yang et al., 2008) and the past shoreline and palaeo-soils records from desert on the Alashan Plateau (Yang and Williams, 2003; Yang and Scuderi, 2010; Yang et al., 2011). In northwestern China, the pollen data from Qinghai lake also showed that the

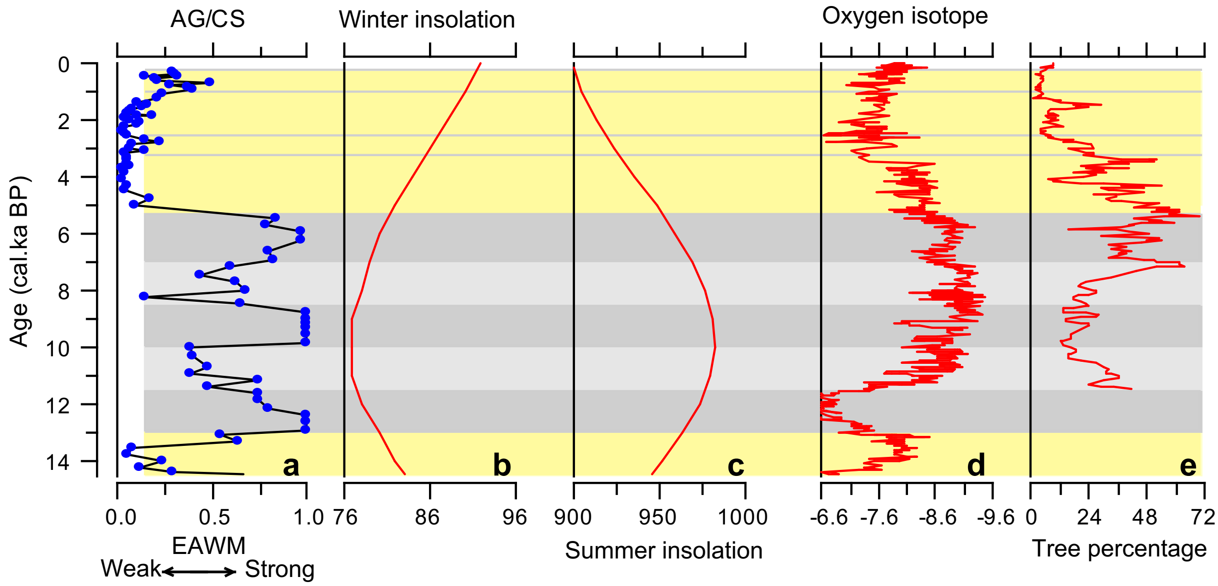

Fig. 9. The relationship between the EAWM and EASM. a. AG/CS ratio; b. December (China winter) insolation at 60°N (W/m^2) (Berger and Loutre, 1991); c. June (China summer) insolation at 60°N (W/m^2) (Berger and Loutre, 1991); d. Stalagmite δ^{18}O records for Dongge cave (Dykoski et al., 2005), as a proxy record of the EASM from southern China; e. Tree percentages from Daihai lake in Inner Mongolia (Xiao et al., 2004), as a proxy record of the EASM in northern China. The shaded areas represent intervals with strong EAWM.

strength of summer monsoon decreased from the early–middle to the late Holocene (Shen et al., 2005). All these data suggest that the EAWM as recorded in the HML region and the EASM as recorded in stalagmites, lakes and desert were controlled, at least during the Holocene, by relatively independent systems (from high latitudes and low latitudes, respectively). Through the Holocene, the retreat of the Northern Hemisphere ice sheet, together with the increase in winter insolation, likely played a substantial role in controlling the EAWM, resulting in a weak EAWM during the late Holocene (Fig. 8c). However, EASM also weakened during the same interval of time as the ITCZ controlled by summer insolation migrated southwards (Fig. 9d) (Dykoski et al., 2005; Fleitmann et al., 2007; Yancheva et al., 2007; Wang et al., 2008c). Our data, when compared with the Chinese stalagmite, lake and desert records, show an in-phase relationship between the EAWM and EASM over the Holocene on orbital time scale (Fig. 9) rather than an anti-phase relationship as suggested by the loess records and HLM Titanium profile (Yancheva et al., 2007).

4.4.2. Millennial time scales

On millennial time scales during the last glacial period, a negative relationship between the EAWM and the EASM is revealed by comparing the EASM and EAWM records from China (Porter and An, 1995; Xiao et al., 1995; Sirocko et al., 1996; An and Porter, 1997; Thompson et al., 1997; Guo et al., 1998; Chen et al., 1999; Oppo and Sun, 2005; Porter and Zhou, 2006; Lu et al., 2007) with the abrupt changes recorded in the North Atlantic (Bond and Lotti, 1995) and ice sheet (The Greenland Summit Ice Cores [CD-ROM], 1997). High-resolution EASM records with accurate chronology, e.g. from stalagmites during the last glacial (Wang et al., 2001), show a close relationship with the oxygen isotopes record from the Greenland ice cores (The Greenland Summit Ice Cores [CD-ROM], 1997), indicating that changes at high latitudes played a very important role in affecting on the EASM during cold periods, such as the Younger Dryas and Heinrich events.

When we compare our record of the EAWM with that of the EASM reconstructed from stalagmite (Dykoski et al., 2005) (Fig. 9d) and pollen records (Xiao et al., 2004) (Fig. 9e), it suggests that the relationship between them was variable spatially and through time. We can establish three different types of relationship: 1) anti-phasing in both northern and southern China during the Last Glacial–Holocene transition, 2) anti-phasing in northern China, but in-phase in southern China during the early–middle Holocene, 3) no clear relationship between them during the late Holocene.

The EAWM as recorded at the HML and the EASM as recorded from pollen data from Daihai Lake in northern China (Xiao et al., 2004) and stalagmite from Dongge cave in southern China (Dykoski et al., 2005) (Fig. 9) during the Last Glacial–Holocene transition between 14.5 and 10 ka are anti-correlated in both northern and southern China. In the interval between c. 13 and 11.7 ka, strong EAWM as recorded by high AG/CS ratio in the HML, is simultaneous with weak EASM, as recorded in Chinese stalagmites from southern (Wang et al., 2001; Dykoski et al., 2005) (Fig. 9d) and northern China (Cai et al., 2008) and high-resolution records from Sihailongwan maar Lake (Parplies et al., 2008; Stebich et al., 2009) and in loess-paleosol sequences from the Chinese Loess Plateau (Zhou et al., 1999, 2001). This interval corresponds to the Younger Dryas cold period.

During the early–middle Holocene between 10 and 5 ka years, the EAWM as recorded at HML is in-phase with the EASM in southern China, but anti-phase with the EASM in northern China. For example, for the 7–5 ka strong EAWM event are not matched by equivalent intervals of weak summer monsoon in southern China as indicated by the stalagmite record of Dongge cave (Dykoski et al., 2005; Wang et al., 2005) (Fig. 9d). By contrast, when we compare the HML diatom record of the EAWM with records of the EASM from northern China, we see that the 7–5 ka strong EAWM event is well matched by an interval of weak summer monsoon as derived from pollen data from Daihai Lake (Xiao et al., 2004) (Fig. 9e). In other places in northern China, the EASM was also shown to have been similarly weak during this period. The high-resolution record from Sihailongwan maar lake in northeastern China showed that summer monsoon rainfall reached a Holocene minima around 6.4 ka (Schettler et al., 2006). TOC data from Dali Lake (Xiao et al., 2008) and multiproxy records from the Tengger desert and Zhuyezhe Lake on the Alashan Plateau (Zhang et al., 2000; Chen et al., 2003) and the sparsity of ^{14}C dates for this time interval (Guo et al., 2000) indicate a weak summer monsoon during this period. A major episode of dry climate conditions with generally low but fluctuating runoff and deposition of aeolian sand lasted for about 2100 yr between 7.5 and 5.4 ka in Juyanze Lake also indicating weak summer monsoon during this period (Hartmann and Wünnemann, 2009). However, in Badain Jaran desert, the highest lake stands, which indicate the wettest period, bracket the interval between 4 and 7.5 ka (Yang et al., 2010).

For the 10–8.5 ka strong EAWM event, although there was no obvious signal in the tree pollen record of Xiao et al. (2004), which shows an overall weak EASM between 11 and 8 ka cal. yrs BP (Fig. 9e), another record from Daihai lake showed that the pollen concentration decreased between 10 and 8.5 ka (Li et al., 2004) while at Hulun Lake the percentages of *Betula* were low (Wen et al., 2010). The Sihailongwan Lake record also showed that aeolian influx of silt-size debris was relatively high during an overall dry period between 9.5 and 8 ka (Schettler et al., 2006). In the Badain Jaran Desert, an end phase of aeolian sand sedimentation was dated to 8200 ± 400 yrs BP by thermoluminescence (Yang and Williams, 2003) while in Hunshandake sandy land an aeolian sand layer was dated to 9300 ± 270 yrs BP (Yang et al., 2008) and also suggest dry periods. Further north, extremely low runoff occurred between 8.9 and 8.1 ka in Juyanze Lake, indicating dry climate conditions (Hartmann and Wünnemann, 2009). Although all these records of dry events are not exactly synchrone with the EAWM events from the HML, they exhibit for these two strong EAWM periods similar millennium scale variability, especially when considering dating uncertainties.

During the late Holocene, the EAWM as interpreted from our diatom data did not show any clear relationship with the EASM derived from the stalagmite and pollen records (Fig. 9). Late Holocene variability in the EASM has been reported from different records (Xiao et al., 2004; Wang et al., 2005) which detail several significant, abrupt changes, but only two weak EAWM events were recorded in HML at about 3000 cal. yrs BP and after 1000 cal. yrs BP (Fig. 9a).

From the above discussion we hypothesize that the relationship between the EAWM and EASM depends on the strength of the EAWM. During the Younger Dryas the EAWM was probably strong enough to impede the EASM front from migrating northward to both northern and southern China, resulting in a weak EASM over both regions consistently with data from southern China (Wang et al., 2001; Dykoski et al., 2005), northern China (Cai et al., 2008), the Chinese Loess Plateau (Zhou et al., 1999, 2001). During the early–middle Holocene, the strengthening of the EAWM during the periods 10–8.5 ka and 7–5.5 ka was unlikely to be as strong as during the Younger Dryas, and would not have displaced the EASM front out of the Chinese mainland especially as the summer insolation was high in the Northern Hemisphere resulting in a strong EASM. These two EAWM events however, were probably strong enough to displace the EASM front out of northern China, which resulted in less precipitation in these regions during these two episodes. This explains the difference we observe between southern and northern China. During the late Holocene, apart from the last 1000 years, the EAWM was so weak that it could not affect the EASM and therefore, there is no clear correlation between the EAWM from the HML and the EASM from the stalagmite and pollen records in that interval.

In summary, the changes in the EAWM and EASM are responsive to climate change at high (AO/NAO) and low latitudes (ITCZ/ENSO), respectively. Our data indicate that the correlation between the EAWM and the EASM is variable, with dependence on the strength of the EAWM. The variability in the spatial correlation between the EAWM and EASM indicate that the influence of the EAWM on the EASM was more significant in northern China than in southern China. This spatial difference in correlation between the EAWM and EASM could explain why the loess-soil sequence recorded weak processional cycle and significant glacial–interglacial cycle of the EASM on the Loess Plateau (Ding et al., 1995; Lu et al., 2004), while by contrast, the stalagmites of southern China recorded significant processional cycle and very weak glacial–interglacial cycle of the EASM (Wang et al., 2008c).

4.5. The correlation between the EAWM and the ASM

Many geological records of the ASM from Australia showed that the ASM was strong in the early–middle Holocene and weak in the late Holocene (Shulmeister, 1991; Shulmeister and Lees, 1995; Wyrwoll and Miller, 2001; Hesse et al., 2004; Magee et al., 2004). The changes in ASM during the Holocene cannot be explained by changes in insolation over the Southern Hemisphere (Fig. 10d and

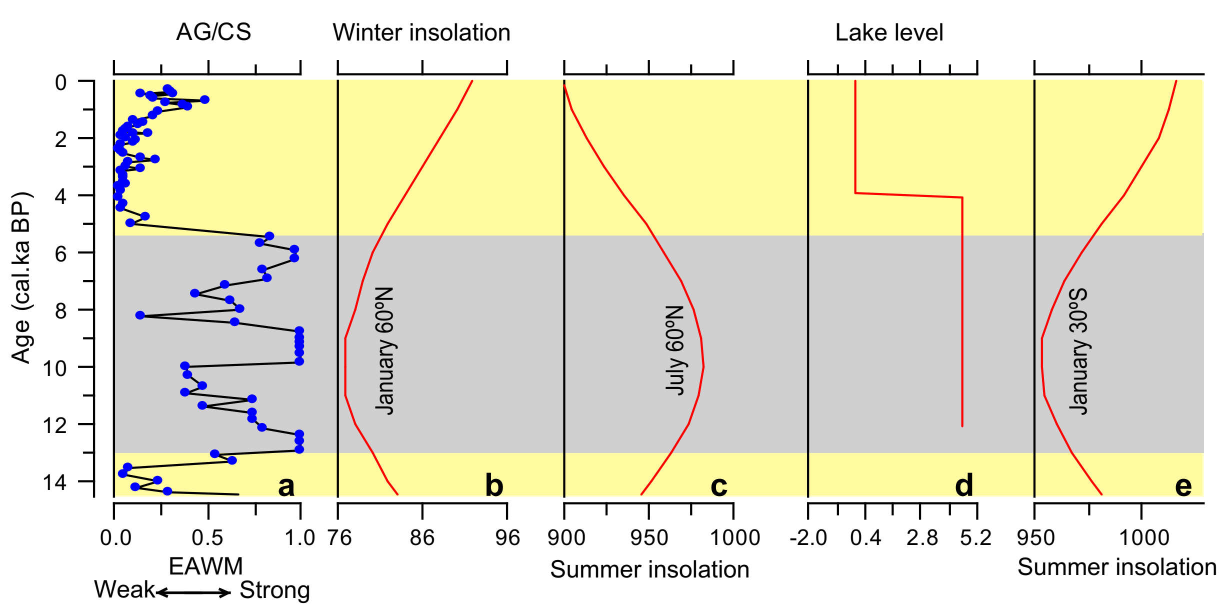

Fig. 10. The relationship between the EAWM and ASM. a. AG/CS ratio. b. December (China winter) insolation at 60°N (W/m^2) (Berger and Loutre, 1991). c. July (China summer) insolation at 60°N (W/m^2) (Berger and Loutre, 1991). d. Eyre Lake (Australia) lake-level record (m, relative to Australian height datum (mean sea level)) (Magee et al., 2004). e. January (Australian summer) insolation at 30°N (W/m^2) (Berger and Loutre, 1991). The shaded areas represent intervals with strong EAWM.

e). An orbital time scale variation in Milankovitch insolation has been widely accepted as a first-order forcing mechanism of monsoon regimes (Kutsbach, 1981; Kutzbach and Street-Perrott, 1985). The variation in rainfall exhibits an inter-hemispheric anti-phasing between southern Brazil and China, because the summer insolation is anti-phased between the Northern and Southern Hemispheres (Wang et al., 2007b). Several hypotheses for the possible factors at play in influencing changes in the ASM over the Holocene have been proposed, including changes in sea level and temperature (Liu et al., 2003), ENSO (Shulmeister and Lees, 1995; Haberle, 2005; Donders et al., 2007; Quigley et al., 2010), as well as summer insolation in the Southern Hemisphere (Wyrwoll et al., 2007).

The EAWM as one of the factors having an influence on the activity of the ASM has been proposed before (Liu and Ding, 1998; Suppiah and Wu, 1998), because meteorological observations show that the low-level northerly and northeasterly air currents can occasionally flow across the Equator and merge with the ASM (Chen et al., 1991). Recently, meteorological data have also indicated that a positive correlation exists between northerly winter winds in the South China Sea and the ASM on an inter-annual time scale (Chase et al., 2003; Wang et al., 2003). The changes in the ASM did not show a positive correlation with the weakening of the EAWM after the 1980s. A possible reason for this discrepancy is that the observed increase in precipitation over Australia during the past 20 years was caused by an increase in aerosols (Rotstayn et al., 2007) and therefore was unrelated to changes in the EAWM.

General Circulation Model (GCM) simulations also suggested that the strength of the ASM is determined by the Northern Hemisphere winter insolation control on the intensity of the SH (Miller et al., 2005) (Fig. 10b), rather than by summer insolation over the Australian continent. However, until now no direct record of the EAWM has been established in support to this hypothesis. The HML diatom record shows that the EAWM shifted from strong to weak from the early to late Holocene, indicating that the EAWM was in-phase with the ASM. This result provides the first direct evidence to support the view that the intensity of the EAWM most likely plays an important role in controlling the strength of the ASM (Suppiah and Wu, 1998; Magee et al., 2004; Miller et al., 2005). This linkage needs to be further explored through the comparison of high-resolution records of both the ASM and EAWM.

5. Conclusions

The diatom record from HML in South China shows that there was a marked shift from strong to weak in the EAWM from the early to late Holocene. Changes in the EAWM were closely linked with high-latitudes climate change on orbital and on millennial time scales during the Holocene. It was also influenced by changes in ENSO. The relationship between the EAWM and EASM show spatial and temporal variability, and is dependent on the strength of the EAWM. Finally, the EAWM was probably one of the most important factors in influencing the changes in the ASM during the early Holocene.

Acknowledgments

We thank Professor Jiaqi Liu and Xiangdong Yang, Dr. Jens Mingram and Lin Wang for helpful discussion and constructive comments, and also thank Li Xianzhong, Peng Zhiming, and Lin Weiguo for their help with field work. Water chemistry analyses were done in IGG-CAS and NIGLAS. We are grateful to Professor John Smol and an anonymous reviewer for their helpful and constructive comments on the manuscript. This research was supported by the National Science Foundation (grants 40572105, 40971121) and National Basic Research Program of China (973 Program) grants 2010CB950200.

References

An, Z.S., Porter, S.C., 1997. Millennial-scale climatic oscillations during the last interglaciation in central China. Geology 25 (7), 603–606.

An, Z.S., Kukla, G., Porter, S.C., Xiao, J.L., 1991a. Late Quaternary dust flow on the Chinese Loess Plateau. Catena 18 (2), 125–132.

An, Z.S., Kukla, G., Porter, S.C., Xiao, J.L., 1991b. Magnetic susceptibility evidence of monsoon variation on the Loess Plateau of central China during the last 130,000 years. Quaternary Research 36 (1), 29–36.

Assaf, G., Gerard, R., Gordon, A.L., 1971. Some mechanisms of oceanic mixing revealed in aerial photographs. Journal of Geophysical Research 76 (27), 6550–6572.

Barnett, T.P., Dumenil, L., Schlese, U., Roeckner, E., 1988. The effect of eurasian snow cover on global climate. Science 239 (4839), 504–507.

Battarbee, R.W., Kneen, M.J., 1982. The use of electronically counted microspheres in absolute diatom analysis. Limnology and Oceanography 27 (1), 184–188.

Battarbee, R.W., Jones, V.J., Flower, B.P., Cameron, N.G., Bennion, H., Carvalho, L., Juggins, S., 2001. Diatoms. In: Smol, J.P., Birks, H.J.B., Last, W.M. (Eds.), Tracking Environmental Change Using Lake Sediments. Kluwer Academic Publishers, Dordrecht, pp. 155–201.

Battarbee, R.W., Grytnes, J.A., Thompson, R., Appleby, P.G., Catalan, J., Korhola, A., Birks, H.J.B., Heegaard, E., Lami, A., 2002. Comparing palaeolimnological and instrumental evidence of climate change for remote mountain lakes over the last 200 years. Journal of Paleolimnology 28 (1), 161–179.

Berger, A., Loutre, M.F., 1991. Insolation values for the climate of the last 10,000,000 years. Quaternary Science Reviews 10 (4), 297–317.

Blomqvist, S., Hakanson, L., 1981. A review on sediment traps in aquatic environments. Archiv für Hydrobiologie 91, 101–132.

Bond, G.C., Lotti, R., 1995. Iceberg discharges into the North Atlantic on millennial time scales during the last glaciation. Science 267 (5200), 1005–1010.

Cai, B.G., Edwards, R.L., Cheng, H., Tan, M., Wang, X., Liu, T.S., 2008. A dry episode during the Younger Dryas and centennial-scale weak monsoon events during the early Holocene: a high-resolution stalagmite record from southeast of the Loess Plateau, China. Geophysical Research Letters 35 (2). doi:10.1029/2007GL030986.

Chan, J.C.L., Li, C.Y., 2004. The East Asia winter monsoon. In: Chang, C.P. (Ed.), East Asian Monsoon. World Scientific Publishing Co. Pet. Ltd, pp. 54–106.

Chang, C.P., Wang, Z., Handon, H., 2006. The Asian winter monsoon. In: Wang, B. (Ed.), The Asian Monsoon. Springer, Chichester, pp. 89–127.

Chase, T.N., Knaff, J.A., Pielke Sr., R.A., Kalnay, E., 2003. Changes in global monsoon circulations since 1950. Natural Hazards 29 (2), 229–254.

Chen, L.X., Zhu, Q.G., Luo, H.B., He, J.H., Dong, M., Feng, Z.Q., 1991. East Asian Monsoon. China Meteorological Press, Beijing, p. 362 (in Chinese).

Chen, F.H., Bloemendal, J., Feng, Z.D., Wang, J.M., Parker, E., Guo, Z.T., 1999. East Asian monsoon variations during Oxygen Isotope Stage 5: evidence from the northwestern margin of the Chinese Loess Plateau. Quaternary Science Reviews 18 (8–9), 1127–1135.

Chen, W., Graf, H.F., Huang, R.H., 2000. The inter-annual variability of East Asian winter monsoon and its relation to the summer monsoon. Advances in Atmosphere Sciences 17 (1), 46–60.

Chen, F.H., Wu, W., Holmes, J.A., Madsen, D.B., Zhu, Y., Jin, M., Oviatt, C.G., 2003. A mid-Holocene drought interval as evidenced by lake desiccation in the Alashan Plateau, Inner Mongolia, China. Chinese Science Bulletin 48 (14), 1401–1410.

Chen, W., Yang, S., Huang, R.H., 2005. Relationship between stationary planetary wave activity and the East Asian winter monsoon. Journal of Geophysical Research-Atmospheres 110 (D14). doi:10.1029/2004JD005669.

Clark, M.P., Serreze, M.C., 2000. Effects of variations in East Asian snow cover on modulating atmospheric circulation over the North Pacific Ocean. Journal of Climate 13 (20), 3700–3710.

Clark, M.P., Serreze, M.C., Robinson, D.A., 1999. Atmospheric controls on Eurasian snow extent. International Journal of Climatology 19 (1), 27–40.

Clemens, S.C., Prell, W.L., Sun, Y.B., 2010. Orbital-scale timing and mechanisms driving Late Pleistocene Indo-Asian summer monsoons: reinterpreting cave speleothem delta^{18}O. Paleoceanography 25. doi:10.1029/2010PA001926.

Clement, A.C., Seager, R., Cane, M.A., 2000. Suppression of El Niño during the mid-Holocene by changes in the Earth's orbit. Paleoceanography 15 (6), 731–737.

Conroy, J.L., Overpeck, J.T., Cole, J.E., Shanahan, T.M., Steinitz-Kannan, M., 2008. Holocene changes in eastern tropical Pacific climate inferred from a Galápagos lake sediment record. Quaternary Science Reviews 27 (11–12), 1166–1180.

D'Arrigo, R., Wilson, R., Panagiotopoulos, F., Wu, B.Y., 2005. On the long-term interannual variability of the East Asian winter monsoon. Geophysical Research Letters 32 (21). doi:10.1029/2005GL023235.

Davis, B.A.S., Brewer, S., Stevenson, A.C., Guiot, J., Contributors, D., 2003. The temperature of Europe during the Holocene reconstructed from pollen data. Quaternary Science Reviews 22 (15–17), 1701–1716.

Ding, Y.H., 1994. Monsoon over China. Kluwer Academic, p. 420.

Ding, Z.L., Liu, T.S., Rutter, N.W., Yu, Z.W., Guo, Z.T., Zhu, R.X., 1995. Ice-volume forcing of East-Asian winter monsoon variations in the past 800,000 years. Quaternary Research 44 (2), 149–159.

Ding, Z.L., Derbyshire, E., Yang, S.L., Yu, Z.W., Xiong, S.F., Liu, T.S., 2002. Stacked 2.6-Ma grain size record from the Chinese loess based on five sections and correlation with the deep-sea delta ^{18}O record. Paleoceanography 17 (3). doi:10.1029/2001PA000725.

Donders, T.H., Haberle, S.G., Hope, G., Wagner, F., Visscher, H., 2007. Pollen evidence for the transition of the eastern Australian climate system from the post-glacial to the present-day ENSO mode. Quaternary Science Reviews 26 (11–12), 1621–1637.

Dyke, A.S., Prest, V.K., 1987. Late Wisconsinian and Holocene history of the Laurentide ice sheet. Géographie Physique et Quaternaire 41, 237–263.

Dykoski, C.A., Edwards, R.L., Cheng, H., Yuan, D.X., Cai, Y.J., Zhang, M.L., Lin, Y.S., Qing, J.M., An, Z.S., Revenaugh, J., 2005. A high-resolution, absolute-dated Holocene and deglacial Asian monsoon record from Dongge cave, China. Earth and Planetary Science Letters 233 (1–2), 71–86.

Fleitmann, D., Burns, S.J., Mangini, A., Mudelsee, M., Kramers, J., Villa, I., Neff, U., Al-Subbary, A.A., Buettner, A., Hippler, D., Matter, A., 2007. Holocene ITCZ and Indian monsoon dynamics recorded in stalagmites from Oman and Yemen (Socotra). Quaternary Science Reviews 26 (1–2), 170–188.

Gong, D.Y., Ho, C.H., 2002. The Siberian High and climate change over middle to high latitude Asia. Theoretical and Applied Climatology 72 (1–2), 1–9.

Gong, D.Y., Wang, S.W., Zhu, J.H., 2001. East Asian winter monsoon and Arctic Oscillation. Geophysical Research Letters 28 (10), 2073–2076.

Guo, Z.T., Liu, T.S., Fedoroff, N., Wei, L.Y., Ding, Z.L., Wu, N.Q., Lu, H.Y., Jiang, W.Y., An, Z.S., 1998. Climate extremes in loess of China coupled with the strength of deep-water formation in the North Atlantic. Global and Planetary Change 18 (3–4), 113–128.

Guo, Z.T., Petit-Maire, N., Kröpelin, S., 2000. Holocene non-orbital climatic events in present-day arid areas of northern Africa and China. Global and Planetary Change 26 (1–3), 97–103.

Haberle, S.G., 2005. A 23,000-yr pollen record from lake Euramoo, wet tropics of NE Queensland, Australia. Quaternary Research 64 (3), 343–356.

Hao, Q.Z., Guo, Z.T., 2005. Spatial variations of magnetic susceptibility of Chinese loess for the last 600 kyr: implications for monsoon evolution. Journal of Geophysical Research-Solid Earth 110 (B12). doi:10.1029/2005JB003765.

Hartmann, K., Wünnemann, B., 2009. Hydrological changes and Holocene climate variations in NW China, inferred from lake sediments of Juyanze palaeolake by factor analyses. Quaternary International 194 (1–2), 28–44.

Hays, J.D., Imbrie, C.W., Shackleton, C., 1976. Variations in the earth's orbit: pacemaker of the ice age. Science 1976, 1121–1132.

Hesse, P.P., Magee, J.W., van der Kaars, S., 2004. Late Quaternary climates of the Australian arid zone: a review. Quaternary International 118–119, 87–102.

Huang, R.H., Zhou, L.T., Chen, W., 2003. The progresses of recent studies on the variabilities of the East Asian monsoon and their causes. Advances in Atmospheric Sciences 20 (1), 55–69.

Huang, R.H., Chen, J.L., Huang, G., 2007. Characteristics and variations of the East Asian monsoon system and its impacts on climate disasters in China. Advances in Atmospheric Sciences 24 (6), 993–1023.

Huang, E., Tian, J., Steinke, S., 2011. Millennial-scale dynamics of the winter cold tongue in the southern South China Sea over the past 26 ka and the East Asian winter monsoon. Quaternary Research 75 (1), 196–204.

Imbrie, C.W., Hays, J.D., Martinson, D.B., McIntyre, A., Mix, A.C., Morley, J.J., Pisias, N.G., Prell, W.L., Shackleton, N.J., 1984. The orbital theory of Pleistocene climate: support from a revised chronology of the marine delta^{18}O record. In: Berger, A., Imbrie, C.W., Hays, J.D., Kukla, G., Saltzman, B. (Eds.), Milankovitch and Climate, Part I. Reidel, Dordrecht, pp. 269–305.

Jhun, J.G., Lee, E.J., 2004. A new East Asian winter monsoon index and associated characteristics of the winter monsoon. Journal of Climate 17 (4), 711–726.

Jiang, W.Y., Guo, Z.T., Sun, X.J., Wu, H.B., Chu, G.Q., Yuan, B.Y., Hatte, C., Guiot, J., 2006. Reconstruction of climate and vegetation changes of Lake Bayanchagan (Inner Mongolia): Holocene variability of the East Asian monsoon. Quaternary Research 65 (3), 411–420.

Jiang, W.Y., Guiot, J., Chu, G.Q., Wu, H.B., Yuan, B.Y., Hatte, C., Guo, Z.T., 2010. An improved methodology of the modern analogues technique for palaeoclimate reconstruction in arid and semi-arid regions. Boreas 39 (1), 145–153.

Kalnay, E., Kanamitsu, M., Kistler, R., Collins, W., Deaven, D., Gandin, L., Iredell, M., Saha, S., White, G., Woollen, J., Zhu, Y., Chelliah, M., Ebisuzaki, W., Higgins, W., Janowiak, J., Mo, K.C., Ropelewski, C., Wang, J., Leetmaa, A., Reynolds, R., Jenne, R., Joseph, D., 1996. The NCEP/NCAR 40-year reanalysis project. Bulletin of the American Meteorological Society 77 (3), 437–471.

Kang, L.H., Chen, W., Wei, K., 2006. The interdecadal variation of winter temperature in China and its relation to anomalies in atmospheric general circulation. Climate and Environmental Research 11 (3), 330–339.

Kilham, P., 1990. Ecology of Melosira species in the Great lakes of Africa. In: Tilzer, M.M., Serruya, C. (Eds.), Large Lakes Ecological Structure and Function. Springer, Berlin, pp. 414–427.

Kilham, S.S., Kilham, P., 1975. *Melosira granulata* (Ehr.) Ralfs: morphology and ecology of a cosmopolitan freshwater diatom. Verhandlungen Internationale Vereinigung für Theoretische und Angewandte Limnologie 19, 2716–2721.

Krammer, K., Lange-Bertalot, H., 1986. Bacillariophyceae. Süsswasserflora von Mitteleuropa, Band 2. Spektrum Akademischer Verlag, Heidelberg, Berlin.

Kukla, G., An, Z.S., 1989. Loess stratigraphy in central China. Palaeogeography, Palaeoclimatology, Palaeoecology 72 (1–2), 203–225.

Kutsbach, J.E., 1981. Monsoon climate of the early Holocene: climate experiment with the earth's orbital parameters for 9000 years ago. Science 214, 59–61.

Kutzbach, J.E., Street-Perrott, F.A., 1985. Milankovitch forcing of fluctuations in the level of tropical lakes from 18 to 0 kyr BP. Nature 317 (6033), 130–134.

Kutzbach, J., Gallimore, R., Harrison, S., Behling, P., Selin, R., Laarif, F., 1998. Climate and biome simulations for the past 21,000 years. Quaternary Science Reviews 17 (6–7), 473–506.

Langmuir, I., 1938. Surface motion of water induced by wind. Science 87 (2250), 119–123.

Lau, K.M., Li, M.T., 1984. The monsoon of East Asia and its global associations a survey. Bulletin of the American Meteorological Society 65 (2), 114–125.

Li, C.Y., 1989. Warmer winter in eastern China and El Niño. Chinese Science Bulletin 34 (21), 1801–1805.

Li, C.Y., 1990. Interaction between anomalous winter monsoon in East Asia and El Niño events. Advances in Atmospheric Sciences 7 (1), 36–46.

Li, C.Y., Mu, M.Q., 2000. Relationship between East Asian winter monsoon, warm pool situation and ENSO cycle. Chinese Science Bulletin 45 (16), 1448–1455.

Li, X.Q., Zhou, J., Shen, J., Weng, C.Y., Zhao, H.L., Sun, Q.L., 2004. Vegetation history and climatic variations during the last 14 ka BP inferred from a pollen record at Daihai Lake, north-central China. Review of Palaeobotany and Palynology 132 (3–4), 195–205.

Li, J.J., Li, J., Wang, L., 2009. The best duration of settling for diatom suspension. Quaternary Sciences 29 (1), 183–184.

Litt, T., Scholzel, C., Kuhl, N., Brauer, A., 2009. Vegetation and climate history in the Westeifel Volcanic Field (Germany) during the past 11,000 years based on annually laminated lacustrine maar sediments. Boreas 38 (4), 679–690.

Liu, T.S., Ding, Z.L., 1998. Chinese loess and the paleomonsoon. Annual Review of Earth and Planetary Sciences 26, 111–145.

Liu, T.S., Ding, Z.L., Rutter, N., 1999. Comparison of Milankovitch periods between continental loess and deep sea records over the last 2.5 Ma. Quaternary Science Reviews 18 (10–11), 1205–1212.

Liu, Z., Otto-Bliesner, B., Kutzbach, J., Li, L., Shields, C., 2003. Coupled climate simulation of the evolution of global monsoons in the Holocene. Journal of Climate 16 (15), 2472–2490.

Liu, Y., Peng, Z.C., Chen, T.G., Wei, G.J., Sun, W.D., Sun, R.Y., He, J.F., Liu, G.J., Chou, C.L., Zartman, R.E., 2008. The decline of winter monsoon velocity in the South China Sea through the 20th century: evidence from the Sr/Ca records in corals. Global and Planetary Change 63 (1), 79–85.

Lu, H., Zhang, F.Q., Liu, X., Duce, R.A., 2004. Periodicities of palaeoclimatic variations recorded by loess-paleosol sequences in China. Quaternary Science Reviews 23 (18–19), 1891–1900.

Lu, H.Y., Wu, N.Q., Liu, K.B., Jiang, H., Liu, T.S., 2007. Phytoliths as quantitative indicators for the reconstruction of past environmental conditions in China II: palaeoenvironmental reconstruction in the Loess Plateau. Quaternary Science Reviews 26 (5–6), 759–772.

Magee, J.W., Miller, G.H., Spooner, N.A., Questiaux, D., 2004. Continuous 150 ky monsoon record from lake Eyre, Australia: insolation-forcing implications and unexpected Holocene failure. Geology 32 (10), 885–888.

Mayewski, P.A., Meeker, L.D., Twickler, M.S., Whitlow, S., Yang, Q.Z., Lyons, W.B., Prentice, M., 1997. Major features and forcing of high-latitude northern hemisphere atmospheric circulation using a 110,000-year-long glaciochemical series. Journal of Geophysical Research-Oceans 102 (C12), 26345–26366.

Mayewski, P.A., Rohling, E.E., Stager, J.C., Karlen, W., Maasch, K.A., Meeker, L.D., Meyerson, E.A., Gasse, F., van Kreveld, S., Holmgren, K., Lee-Thorp, J., Rosqvist, G., Rack, F., Staubwasser, M., Schneider, R.R., Steig, E.J., 2004. Holocene climate variability. Quaternary Research 62 (3), 243–255.

Meeker, L.D., Mayewski, P.A., 2002. A 1400-year high-resolution record of atmospheric circulation over the North Atlantic and Asia. Holocene 12 (3), 257–266.

Miller, G., Mangan, J., Pollard, D., Thompson, S., Felzer, B., Magee, J., 2005. Sensitivity of the Australian monsoon to insolation and vegetation: implications for human impact on continental moisture balance. Geology 33 (1), 65–68.

Mingram, J., Schettler, G., Nowaczyk, N.R., Luo, X., Lu, H.Y., Liu, J.Q., Negendank, J.F.W., 2004. The Huguang maar Lake a high-resolution record of palaeoenvironmental and palaeoclimatic changes over the last 78,000 years from South China. Quaternary International 122 (1), 85–107.

Moy, C.M., Seltzer, G.O., Rodbell, D.T., Anderson, D.M., 2002. Variability of El Niño/Southern Oscillation activity at millennial timescales during the Holocene epoch. Nature 420 (6912), 162–165.

Oliver, J.E., 2005. Encyclopedia of World Climatology. Springer, Dordrecht, The Netherlands, p. 854.

Oppo, D.W., Sun, Y.B., 2005. Amplitude and timing of sea-surface temperature change in the northern South China Sea: dynamic link to the East Asian monsoon. Geology 33 (10), 785–788.

Panagiotopoulos, F., Shahgedanova, M., Hannachi, A., Stephenson, D.B., 2005. Observed trends and teleconnections of the Siberian High: a recently declining center of action. Journal of Climate 18 (9), 1411–1422.

Parplies, J., Lucke, A., Vos, H., Mingram, J., Stebich, M., Radtke, U., Han, J., Schleser, G.H., 2008. Late glacial environment and climate development in northeastern China derived from geochemical and isotopic investigations of the varved sediment record from Lake Sihailongwan (Jilin Province). Journal of Paleolimnology 40 (1), 471–487.

Pilskaln, C.H., Johnson, T.C., 1991. Seasonal signals in Lake Malawi sediments. Limnology and Oceanography 36 (3), 544–557.

Porter, S.C., 2001. Chinese loess record of monsoon climate during the last glacial-interglacial cycle. Earth-Science Reviews 54 (1–3), 115–128 (special issue).

Porter, S.C., An, Z.S., 1995. Correlation between climate events in the North Atlantic and China during the last glaciation. Nature 375 (6529), 305–308.

Porter, S.C., Zhou, W.J., 2006. Synchronism of Holocene East Asian monsoon variations and North Atlantic drift-ice tracers. Quaternary Research 65 (3), 443–449.

Quigley, M.C., Horton, T., Hellstrom, J.C., Cupper, M.L., Sandiford, M., 2010. Holocene climate change in arid Australia from speleothem and alluvial records. Holocene 20 (7), 1093–1104.

Reynolds, C., 2006. Ecology of Phytoplankton. Cambridge University Press, New York, p. 535.

Rodbell, D.T., Seltzer, G.O., Anderson, D.M., Abbott, M.B., Enfield, D.B., Newman, J.H., 1999. An similar to 15,000-year record of El Niño-driven alluviation in southwestern Ecuador. Science 283 (5401), 516–520.

Rotstayn, L.D., Cai, W.J., Dix, M.R., Farquhar, G.D., Feng, Y., Ginoux, P., Herzog, M., Ito, A., Penner, J.E., Roderick, M.L., Wang, M.H., 2007. Have Australian rainfall and cloudiness increased due to the remote effects of Asian anthropogenic aerosols? Journal of Geophysical Research-Atmospheres 112 (D9). doi:10.1029/2006JD007712.

Ruddiman, W.F., Raymo, M.E., Martinson, D.B., Clement, B.M., Backman, J., 1989. Pleistocene evolution: Northern Hemisphere ice sheets and the North Atlantic Ocean. Paleoceanography 4 (4), 353–412.

Rühland, K., Priesnitz, A., Smol, J.P., 2003. Paleolimnological evidence from diatoms for recent environmental changes in 50 lakes across Canadian arctic treeline. Arctic, Antarctic, and Alpine Research 35, 110–123.

Schettler, G., Liu, Q., Mingram, J., Stebich, M., Dulski, P., 2006. East-Asian monsoon variability between 15,000 and 2000 cal. yr BP recorded in varved sediments of Lake Sihailongwan (northeastern China, Long Gang volcanic field). Holocene 16 (8), 1043–1057.

Scott, J.T., Myer, G.E., Stewart, R., Walther, E.G., 1969. On the mechanism of Langmuir circulations and their role in epilimnion mixing. Limnology and Oceanography 14 (4), 493–503.

Shackleton, C., Berger, A., Peltier, W.R., 1990. An alternative astronomical calibration of the lower Pleistocene time scale based on ODP site 677. Philosophical Transactions of the Royal Society, Edinburgh 81, 251–261.

Shen, J., Liu, X.Q., Wang, S.M., Matsumoto, R., 2005. Palaeoclimatic changes in the Qinghai Lake area during the last 18,000 years. Quaternary International 136 (1), 131–140.

Shulmeister, J., 1991. A Holocene pollen record from lowland tropical Australia. The Holocene 2 (2), 107–116.

Shulmeister, J., Lees, B.G., 1995. Pollen evidence from tropical Australia for the onset of an ENSO-dominated climate at c. 4000 BP. Holocene 5 (1), 10–18.

Sirocko, F., GarbeSchonberg, D., McIntyre, A., Molfino, B., 1996. Teleconnections between the subtropical monsoons and high-latitude climates during the last deglaciation. Science 272 (5261), 526–529.

Sorvari, S., Korhola, A., Thompson, R., 2002. Lake diatom response to recent Arctic warming in Finnish Lapland. Global Change Biology 8 (2), 153–163.

Stebich, M., Mingram, J., Han, J.T., Liu, J.Q., 2009. Late Pleistocene spread of (cool-) temperate forests in Northeast China and climate changes synchronous with the North Atlantic region. Global and Planetary Change 65 (1–2), 56–70.

Suppiah, R., Wu, X.G., 1998. Surges, cross-equatorial flows and their links with the Australian summer monsoon circulation and rainfall. Australian Meteorological Magazine 47 (2), 113–130.

Tan, M., 2009. Circulation effect: climatic significance of the short term variability of the oxygen isotopes in stalagmites from monsoonal China - dialogue between paleoclimate records and modern climate research. Quaternary Sciences 29 (5), 851–862 (in Chinese, with English Abstr.).

The Greenland Summit Ice Cores [CD-ROM], 1997. Available from the National Snow and Ice Data Center, University of Colorado at Boulder, and the World Data Center-A for Paleoclimatology, National Geophysical Data Center, Boulder, CO. Also available online at: www.ngdc.noaa.gov/paleo/icecore/greenland/summit/index.html.

Thompson, D.W.J., Wallace, J.M., 1998. The Arctic Oscillation signature in the wintertime geopotential height and temperature fields. Geophysical Research Letters 25 (9), 1297–1300.

Thompson, L.G., Yao, T., Davis, M.E., Henderson, K.A., Mosley-Thompson, E., Lin, P.N., Beer, J., Synal, H.A., Cole-Dai, J., Bolzan, J.F., 1997. Tropical climate instability: the last glacial cycle from a Qinghai-Tibetan ice core. Science 276 (5320), 1821–1825.

Tian, J., Huang, E.Q., Pak, D.K., 2010. East Asian winter monsoon variability over the last glacial cycle: insights from a latitudinal sea-surface temperature gradient across the South China Sea. Palaeogeography, Palaeoclimatology, Palaeoecology 292 (1–2), 319–324.

Tudhope, A.W., Chilcott, C.P., McCulloch, M.T., Cook, E.R., Chappell, J., Ellam, R.M., Lea, D.W., Lough, J.M., Shimmield, G.B., 2001. Variability in the El Niño–Southern Oscillation through a glacial-interglacial cycle. Science 291 (5508), 1511–1517.

Wallace, J.M., 2000. North Atlantic Oscillation/annular mode: two paradigms - one phenomenon. Quarterly Journal of the Royal Meteorological Society 126 (564), 791–805.

Wang, L., Chen, W., 2010. How well do existing indices measure the strength of the East Asian winter monsoon? Advances in Atmospheric Sciences 27 (4), 855–870.

Wang, B., Wu, R.G., Fu, X.H., 2000. Pacific-East Asian teleconnection: how does ENSO affect East Asian climate? Journal of Climate 13 (9), 1517–1536.

Wang, Y.J., Cheng, H., Edwards, R.L., An, Z.S., Wu, J.Y., Shen, C.C., Dorale, J.A., 2001. A high-resolution absolute-dated Late Pleistocene monsoon record from Hulu Cave, China. Science 294 (5550), 2345–2348.

Wang, B., Clemens, S.C., Liu, P., 2003. Contrasting the Indian and East Asian monsoons: implications on geologic timescales. Marine Geology 201 (1–3), 5–21.

Wang, Y.J., Cheng, H., Edwards, R.L., He, Y.Q., Kong, X.G., An, Z.S., Wu, J.Y., Kelly, M.J., Dykoski, C.A., Li, X.D., 2005. The Holocene Asian monsoon: links to solar changes and North Atlantic climate. Science 308 (5723), 854–857.

Wang, S.Y., Lu, H.Y., Liu, J.Q., Negendank, J.F.W., 2007a. The early Holocene optimum inferred from a high-resolution pollen record of Huguangyan Maar Lake in southern China. Chinese Science Bulletin 52 (20), 2829–2836.

Wang, X.F., Auler, A.S., Edwards, R.L., Cheng, H., Ito, E., Wang, Y.J., Kong, X.G., Solheid, M., 2007b. Millennial-scale precipitation changes in southern Brazil over the past 90,000 years. Geophysical Research Letters 34 (23). doi:10.1029/2007GL031149.

Wang, L., Chen, W., Huang, R.H., 2008a. Interdecadal modulation of PDO on the impact of ENSO on the East Asian winter monsoon. Geophysical Research Letters 35 (20). doi:10.1029/2008GL035287.

Wang, L., Lu, H.Y., Liu, J.Q., Gu, Z.Y., Mingram, J., Chu, G.Q., Li, J.J., Rioual, P., Negendank, J.F.W., Han, J.T., Liu, T.S., 2008b. Diatom-based inference of variations in the strength of Asian winter monsoon winds between 17,500 and 6000 calendar years BP. Journal of Geophysical Research-Atmospheres 113 (D21). doi:10.1029/2008JD010145.

Wang, Y.J., Cheng, H., Edwards, R.L., Kong, X.G., Shao, X.H., Chen, S.T., Wu, J.Y., Jiang, X.Y., Wang, X.F., An, Z.S., 2008c. Millennial- and orbital-scale changes in the east Asian monsoon over the past 224,000 years. Nature 451 (7182), 1090–1093.

Wang, L., Chen, W., Zhou, W., Huang, R.H., 2009. Interannual variations of East Asian trough Axis at 500 hPa and its association with the East Asian winter monsoon pathway. Journal of Climate 22 (3), 600–614.

Wen, R.L., Xiao, J.L., Chang, Z.G., Zhai, D.Y., Xu, Q.H., Li, Y.C., Itoh, S., Lomtatidze, Z., 2010. Holocene climate changes in the mid-high-latitude-monsoon margin reflected by the pollen record from Hulun Lake, northeastern Inner Mongolia. Quaternary Research 73 (2), 293–303.

Wu, B.Y., Wang, J., 2002. Winter Arctic Oscillation, Siberian High and East Asian winter monsoon. Geophysical Research Letters 29 (19). doi:10.1029/2002GL015373.

Wyrwoll, K.H., Miller, G.H., 2001. Initiation of the Australian summer monsoon 14,000 years ago. Quaternary International 83–85, 119–128.

Wyrwoll, K.H., Liu, Z.Y., Chen, G.S., Kutzbach, J.E., Liu, X.D., 2007. Sensitivity of the Australian summer monsoon to tilt and precession forcing. Quaternary Science Reviews 26 (25–28), 3043–3057.

Xiao, J.L., Porter, S.C., An, Z.S., Kumai, H., Yoshikawa, S., 1995. Grain-size of quartz as an indicator of winter monsoon strength on the Loess Plateau of central China during the last 130,000-yr. Quaternary Research 43 (1), 22–29.

Xiao, J.L., Xu, Q., Nakamura, T., Yang, X., Liang, W., Inouchi, Y., 2004. Holocene vegetation variation in the Daihai Lake region of north-central China: a direct indication of the Asian monsoon climatic history. Quaternary Science Reviews 23 (14–15), 1669–1679.

Xiao, J.L., Si, B., Zhai, D., Itoh, S., Lomtatidze, Z., 2008. Hydrology of Dali lake in central-eastern Inner Mongolia and Holocene East Asian monsoon variability. Journal of Paleolimnology 40 (1), 519–528.

Xu, J.J., Chan, J.C.L., 2001. The role of the Asian-Australian monsoon system in the onset time of El Niño events. Journal of Climate 14 (3), 418–433.

Yancheva, G., Nowaczyk, N.R., Mingram, J., Dulski, P., Schettler, G., Negendank, J.F.W., Liu, J.Q., Sigman, D.M., Peterson, L.C., Haug, G.H., 2007. Influence of the intertropical convergence zone on the East Asian monsoon. Nature 445 (7123), 74–77.

Yang, S.L., Ding, Z.L., 2008. Advance-retreat history of the East-Asian summer monsoon rainfall belt over northern China during the last two glacia-intergalcial cycles. Earth and Planetary Science Letters 274 (3–4), 499–510.

Yang, X., Scuderi, L., 2010. Hydrological and climatic changes in deserts of China since the Late Pleistocene. Quaternary Research 73 (1), 1–9.

Yang, X., Williams, M., 2003. The ion chemistry of lakes and late Holocene desiccation in the Badain Jaran Desert, Inner Mongolia, China. Catena 51 (1), 45–60.

Yang, X., Zhu, B., Wang, X., Li, C., Zhou, Z., Chen, J., Wang, X., Yin, J., Lu, Y., 2008. Late Quaternary environmental changes and organic carbon density in the Hunshandake Sandy Land, eastern Inner Mongolia, China. Global and Planetary Change 61 (1), 70–78.

Yang, X., Ma, N., Dong, J., Zhu, B., Xu, B., Ma, Z., Liu, J., 2010. Recharge to the interdune lakes and Holocene climatic changes in the Badain Jaran Desert, western China. Quaternary Research 73 (1), 10–19.

Yang, X., Scuderi, L., Paillou, P., Liu, Z., Li, H., Ren, X., 2011. Quaternary environmental changes in the drylands of China - a critical review. Quaternary Science Reviews 30 (23–24), 3219–3536.

Zhang, J.C., Lin, Z.G., 1992. Climate of China. Wiley, p. 376.

Zhang, H.C., Ma, Y.Z., Wünnemannc, B., Pachur, H.J., 2000. A Holocene climatic record from arid northwestern China. Palaeogeography, Palaeoclimatology, Palaeoecology 162 (3–4), 389–401.

Zhou, W.J., Head, M.J., Lu, X.F., An, Z.S., Jull, A.J.T., Donahue, D., 1999. Teleconnection of climatic events between East Asia and polar, high latitude areas during the last deglaciation. Palaeogeography, Palaeoclimatology, Palaeoecology 152 (1–2), 163–172.

Zhou, W.J., Head, M.J., An, Z.S., De Deckker, P., Liu, Z.Y., Liu, X.D., Lu, X.F., Donahue, D., Jull, A.J.T., Beck, J.W., 2001. Terrestrial evidence for a spatial structure of tropical-polar interconnections during the Younger Dryas episode. Earth and Planetary Science Letters 191 (3–4), 231–239.

Zhou, H.Y., Guan, H.Z., Chi, B.Q., 2007. Record of winter monsoon strength. Nature 450 (7168), E10–E11.

Zhou, H.Y., Wang, B., Guan, H.Z., Lai, Y., You, C., Wang, J.L., Yang, H., 2009. Constraints from strontium and neodymium isotopic ratios and trace elements on the sources of the sediments in Lake Huguang Maar. Quaternary Research 72 (2), 289–300.